The Programmed Death-1 Ligand 1:B7-1 Pathway Restrains Diabetogenic Effector T Cells In Vivo

Alison M. Paterson, Keturah E. Brown, Mary E. Keir, Vijay K. Vanguri, Leonardo V. Riella, Anil Chandraker, Mohamed H. Sayegh, Bruce R. Blazar, Gordon J. Freeman and Arlene H. Sharpe

J Immunol; Prepublished online 22 June 2011;
doi:10.4049/jimmunol.1003496
http://www.jimmunol.org/content/early/2011/06/22/jimmunol.1003496

The Journal of Immunology is published twice each month by
The American Association of Immunologists, Inc.,
9650 Rockville Pike, Bethesda, MD 20814-3994.

Print ISSN: 0022-1767 Online ISSN: 1550-6606.

Published June 22, 2011, doi:10.4049/jimmunol.1003496

The Programmed Death-1 Ligand 1:B7-1 Pathway Restrains Diabetogenic Effector T Cells In Vivo

Alison M. Paterson,* Keturah E. Brown,* Mary E. Keir,* Vijay K. Vanguri,† Leonardo V. Riella,‡ Anil Chandraker,‡ Mohamed H. Sayegh,‡ Bruce R. Blazar,§,¶ Gordon J. Freeman,‖,# and Arlene H. Sharpe*

Programmed death-1 ligand 1 (PD-L1) is a coinhibitory molecule that negatively regulates multiple tolerance checkpoints. In the NOD mouse model, PD-L1 regulates the development of diabetes. PD-L1 has two binding partners, programmed death-1 and B7-1, but the significance of the PD-L1:B7-1 interaction in regulating self-reactive T cell responses is not yet clear. To investigate this issue in NOD mice, we have compared the effects of two anti–PD-L1 Abs that have different blocking activities. Anti–PD-L1 mAb 10F.2H11 sterically and functionally blocks only PD-L1:B7-1 interactions, whereas anti–PD-L1 mAb 10F.9G2 blocks both PD-L1:B7-1 and PD-L1:programmed death-1 interactions. Both Abs had potent, yet distinct effects in accelerating diabetes in NOD mice: the single-blocker 10F.2H11 mAb was more effective at precipitating diabetes in older (13-wk-old) than in younger (6- to 7-wk-old) mice, whereas the dual-blocker 10F.9G2 mAb rapidly induced diabetes in NOD mice of both ages. Similarly, 10F.2H11 accelerated diabetes in recipients of T cells from diabetic, but not prediabetic mice, whereas 10F.9G2 was effective in both settings. Both anti–PD-L1 mAbs precipitated diabetes in adoptive transfer models of $CD4^+$ and $CD8^+$ T cell-driven diabetes. Taken together, these data demonstrate that the PD-L1:B7-1 pathway inhibits potentially pathogenic self-reactive effector $CD4^+$ and $CD8^+$ T cell responses in vivo, and suggest that the immunoinhibitory functions of this pathway may be particularly important during the later phases of diabetogenesis. ***The Journal of Immunology*****, 2011, 187: 000–000.**

Programmed death-1 (PD-1; CD279) is an inhibitory receptor that attenuates TCR signaling by recruitment of phosphatases (1, 2). Interactions between PD-1 and its ligands programmed death-1 ligand 1 (PD-L1; B7-H1; CD274) and PD-L2 (B7-DC; CD273) deliver inhibitory signals that regulate T cell activation, tolerance, and immune-mediated tissue damage (3–8). PD-1:PD-L interactions regulate multiple tolerance checkpoints that prevent autoimmunity (3, 4). In addition, the PD-1:PD-L1 pathway plays a key role in controlling host defenses aimed at eradicating microbial pathogens and tumors (3, 9) and is an essential mediator of T cell exhaustion, contributing to lack of viral control during chronic infections as well as to T cell unresponsiveness in the suppressive tumor microenvironment (10, 11).

*Department of Pathology, Harvard Medical School, Boston, MA 02115; †Department of Pathology, University of Massachusetts Medical School, Worcester, MA 01655; ‡Renal Division, Transplantation Research Center, Brigham & Women's Hospital and Children's Hospital, Harvard Medical School, Boston, MA 02115; §Division of Blood and Marrow Transplantation, Department of Pediatrics, University of Minnesota, Minneapolis, MN 55455; ¶Masonic Cancer Center, University of Minnesota, Minneapolis, MN 55455; ‖Department of Medical Oncology, Dana-Farber Cancer Institute, Boston, MA 02115; and #Department of Medicine, Harvard Medical School, Boston, MA 02115

Received for publication October 21, 2010. Accepted for publication May 9, 2011.

This work was supported by National Multiple Sclerosis Society Grant FG 1805-A-1 (to A.M.P.) and National Institutes of Health Grants PO1 AI56299 (to A.H.S., M.H.S., B.R.B., and G.J.F.), R01 AI051559 (to M.H.S. and G.J.F.), PO1 AI39671 (to A.H.S.), and R37 A1038310 (to A.H.S.).

Address correspondence and reprint requests to Dr. Arlene H. Sharpe, Department of Pathology, Harvard Medical School, 77 Avenue Louis Pasteur, NRB-837, Boston, MA 02115. E-mail address: arlene_sharpe@hms.harvard.edu

The online version of this article contains supplemental material.

Abbreviations used in this article: 7-AAD, 7-amino-actinomycin D; PD-1, programmed death-1; PD-L1, programmed death-1 ligand 1.

PD-L1 is constitutively expressed on mouse B cells, dendritic cells, macrophages, and T cells, and is further upregulated upon their activation (12). PD-L1 also is expressed on a variety of nonhematopoietic cell types, including vascular endothelial cells and pancreatic islet cells (3, 13, 14). The broad expression of PD-L1 on hematopoietic and nonhematopoietic cells suggests that PD-L1 may have important roles in inhibiting immune responses in both lymphoid and nonlymphoid organs. Our bone marrow chimera studies revealed that PD-L1 expression on nonhematopoetic cells can shield the pancreas from immune-mediated tissue damage in the NOD diabetes model (15).

We recently identified B7-1 (CD80), a ligand for CD28 and CTLA-4, as a second binding partner for PD-L1 in mice (16) and humans (17, 18). B7-1 associates with PD-L1 with an affinity of ~1.4 μM, 2- to 3-fold higher than that of B7-1 for CD28, and about one-third the affinity of PD-L1 for PD-1 (16). The interaction between B7-1 and PD-L1 bidirectionally inhibits T cell proliferation and cytokine production in vitro (16).

The individual contributions of PD-L1:B7-1 and PD-L1:PD-1 interactions in controlling T cell responses in vivo are not yet understood. Studies with PD-L1–deficient mice cannot distinguish between the absence of PD-L1:B7-1 or PD-L1:PD-1 interactions. In addition, we have found that most commonly used anti–PD-L1 mAbs block the interactions of PD-L1 with both PD-1 and B7-1. Thus, it is unclear whether functions previously attributed to PD-1:PD-L1 interactions are in fact due to B7-1:PD-L1 interactions, at least in part. Using an avidity-based adhesion assay (16), we characterized a panel of anti-mouse PD-L1 mAbs, and identified a dual-blocker mAb (which prevents binding of PD-L1 to PD-1 and B7-1) and a single-blocker mAb (which prevents binding of PD-L1 to B7-1 only), 10F.9G2 and 10F.2H11, respectively. In this study, we use the different blocking properties of these mAbs to compare the functional effects of both PD-L1 pathways in vivo, and elucidate a function for the novel PD-L1:B7-1 pathway.

We have chosen to compare the consequences of administering these two types of anti–PD-L1 mAbs to NOD mice, because we and others have demonstrated a critical role for PD-L1 in controlling self-reactive T cell responses during NOD diabetes (14, 15). Blockade of PD-L1 with an anti–PD-L1 mAb (which is a dual blocker) led to rapid onset of diabetes in 1- and 10-wk-old prediabetic NOD mice (14). We found that PD-L1–deficient NOD mice develop markedly accelerated diabetes (15), and that PD-L1 can regulate the initial activation of potentially pathogenic T cells as well as the responses of pathogenic effector T cells (19, 20). Furthermore, diabetes is accelerated when either of the PD-L1–binding partners PD-1 or B7-1 is blocked or eliminated in NOD mice (14, 21, 22). Because PD-L1, PD-1, and B7-1 all have important roles in controlling NOD diabetes, the PD-L1:B7-1 pathway may regulate the initiation and/or progression of autoimmune diabetes. As PD-L1$^{-/-}$, PD-1$^{-/-}$, and B7-1$^{-/-}$ NOD mice all develop accelerated diabetes, it is challenging to use these mice as tools to dissect PD-L1:B7-1 versus PD-L1:PD-1 interactions in vivo. In this study, we have compared the functional effects of anti–PD-L1 mAbs that can block both PD-L1:B7-1 and PD-L1:PD-1 interactions (10F.9G2), or only PD-L1:B7-1 interactions (10F.2H11) during the development of NOD diabetes. Our studies show that B7-1:PD-L1 interactions, as well as PD-1:PD-L1 interactions, can restrain the responses of self-reactive T cells in vivo, and suggest that B7-1:PD-L1 interactions may be particularly important for regulating potentially pathogenic self-reactive effector T cells.

Materials and Methods

Mice

NOD/ShiltJ (NOD), NOD.CB17-Prkdc^{Scid}/J (NOD SCID), and NOD.Cg-Tg(TcraTcrbNY8.3)1Pesa/Dvs/J (8.3 NOD) mice were purchased from The Jackson Laboratory (Bar Harbor, ME). Additional 8.3 NOD mice were a gift from M. Anderson (Diabetes Center, University of California, San Francisco, San Francisco, CA). BDC2.5 NOD and Foxp3-GFP NOD mice were obtained from the Juvenile Diabetes Research Foundation Center on Immunological Tolerance in Type-1 Diabetes (Boston, MA) and bred to generate BDC2.5 Foxp3-GFP NOD mice. Transgenic mice that constitutively overexpress PD-1 on T cells (PD-1A transgenic mice) have been reported previously (23). Harvard Medical School is accredited by the American Association of Accreditation of Laboratory Animal Care. Mice were maintained and used according to institutional and National Institutes of Health guidelines in a specific pathogen-free barrier facility. Only female mice were used in these experiments. Mice were monitored for high urine glucose (Diastix; Bayer, Elkhart, IN). Positive glucosuria readings were confirmed by blood glucose measurement (Ascensia Contour; Bayer). Diabetes was confirmed by two consecutive blood glucose measurements of ≥250 mg/dl. Mice were sacrificed at the indicated time points or upon the second hyperglycemia reading.

For ex vivo analyses, pancreatic lymph nodes, spleen, and pancreata were removed, and single-cell suspensions were prepared using a 70-μm cell strainer (BD Biosciences, San Jose, CA). Pancreata were treated with collagenase P (Sigma-Aldrich, St. Louis, MO) prior to dissociation.

For histology, pancreata were fixed in 10% buffered formalin, dehydrated in graded alcohols and xylenes, embedded in paraffin, and stained with H&E. Islets were scored, in a blinded fashion, as peri-insulitic if mononuclear cells were surrounding the islet, insulitic if mononuclear cells were invading the islets, or normal if no mononuclear cells were surrounding or within the islets. Slides with fewer than five islets were excluded from analysis. At least four slides, from individual mice, were analyzed per group.

Abs and flow cytometry

Anti–PD-L1 Abs 10F.9G2 (24) and 10F.2H11 (16) (both rat IgG2b) and rat IgG2b isotype control Ab (clone LTF-2; BioXCell, West Lebanon, NH) were dialyzed against PBS, sterile filtered, tested for endotoxin (*Limulus* amebocyte lysate assay), and found to have <2 EU/mg. For in vivo Ab administration, mice were given 0.5 mg Ab on day 0, followed by 0.25 mg on days 2, 4, 6, 8, and 10 (all i.p.). If a mouse became diabetic before day 10, treatment was ceased.

For surface staining, 10F.9G2, 10F.2H11, and isotype control Abs were directly conjugated to Alexa Fluor 488 using a protein-labeling kit (Invitrogen, Eugene, OR) or were detected using goat anti-rat IgG (H + L) conjugated to Alexa Fluor 647 (Invitrogen). mAbs specific for CD3 (145-2C11), CD8 (53-6.7), CD4 (RM4-5), CD62L (MEL-14), CD44 (IM7), IFN-γ (XMG1.2), TNF-α (MP6-XT22), and PD-L1 (MIH5) were used for surface or intracellular staining (BioLegend, San Diego, CA). For cell surface stains, single-cell suspensions were preincubated with purified anti-mouse CD16/32 Fc block (2 μg/ml; eBioscience, San Diego, CA) for 10 min, incubated for 30 min in 1–2 μg/ml fluorochrome-conjugated Ab, and then washed twice in 1% heat-inactivated FCS/2 mM EDTA/PBS. For intracellular staining, cells were stimulated for 5 h in 100 ng/ml PMA and 500 ng/ml ionomycin (both Sigma-Aldrich) in the presence of GolgiStop (BD Biosciences, San Jose, CA). Cells were then stained for surface markers as above and processed using a Cytofix/Cytoperm fixation/permeabilization solution kit (BD Biosciences), according to the manufacturer's instructions. Positive gates were defined using appropriate isotype control Abs. For CFSE-dilution studies (see below), cells were stained with anti-CD4 and anti-CD8 and with 7-amino-actinomycin D (7-AAD; BioLegend), according to the manufacturer's instructions.

For cross-blocking studies, cells were incubated for 30 min with purified 10F.9G2, 10F.2H11, or rat IgG2b (20 μg/ml), washed, and then stained with fluorescently conjugated mAb using the above surface-staining procedure. Cell analyses were performed using FACSCalibur or LSR II flow cytometers (BD Biosciences) and FlowJo software (Tree Star, Ashland, OR).

In vitro T cell activation

Plates (96-well flat bottom; BD Biosciences) were coated overnight at 4°C with 4 μg/ml anti-CD3 (clone 2C11; BD Biosciences) and 20 μg/ml mouse PD-L1–human Fc IgG1 fusion protein (R&D Systems, Minneapolis, MN) or control human Fc IgG1 (BioXCell) diluted in PBS. The next day, plates were washed three times with PBS and then incubated at 37°C for 3 h with a range of concentrations of 10F.9G2, 10F.2H11, or rat IgG2b isotype control Abs diluted in PBS. Plates were then washed three times with PBS, and 1×10^5 T cells (CD4$^+$ and CD8$^+$) from PD-1A transgenic mice were added. CD4$^+$ and CD8$^+$ T cells were simultaneously isolated by positive selection using MACS (Miltenyi Biotec, Auburn, CA) beads and columns and labeled with Vybrant CFDA SE (CFSE) Cell Tracer Kit (Invitrogen). After 3 d, proliferation was assessed by flow cytometry, and supernatants were harvested for IFN-γ analysis.

Adoptive transfers

For adoptive transfers, NOD donors were confirmed to be euglycemic (~100–120 mg/dl) or diabetic (>250 mg/dl) by blood glucose measurement. Donor inguinal, brachial, axillary, and pancreatic lymph nodes and spleens were isolated, pooled, and subjected to the indicated cell isolation procedures. For adoptive transfer of total NOD T cells, CD4$^+$ and CD8$^+$ T cells were simultaneously isolated by positive selection using MACS beads and columns (Miltenyi Biotec, Auburn, CA). T cells ($9–10 \times 10^6$) from prediabetic or diabetic NOD donors were transferred by i.v. injection into NOD SCID recipients. For adoptive transfer of BDC2.5 T cells, CD4$^+$ T cells were isolated from BDC2.5 Foxp3-GFP NOD mice by MACS (Miltenyi Biotec) and sorted using a FACS Aria cell sorter (BD Biosciences), and 2×10^4 CD4$^+$Foxp3-GFP$^-$ T cells were transferred i.v. into NOD SCID recipients. For adoptive transfer of 8.3 NOD T cells, CD8$^+$ T cells from 8.3 NOD mice were isolated by MACS, and $4–6 \times 10^6$ T cells were transferred i.v. into NOD SCID recipients. For all transfer experiments, T cell purity was assessed by flow cytometry and was consistently >96% after MACS isolation and >99% after sorting.

ELISA

For PD-L1 studies, Nunc ELISA plates (Thermo Scientific, Roskilde, Denmark) were coated with anti–PD-L1 mAbs overnight in PBS. The following day, plates were blocked with 2% BSA/PBS for 1 h at 37°C and then incubated with mouse PD-L1–human Fc IgG1 fusion protein (R&D Systems) or control human Fc IgG1 (BioXCell) at 1 μg/ml for 3 h at 37°C. Plates were washed and incubated with biotinylated anti-human IgG (Jackson ImmunoResearch Laboratories, West Grove, PA) for 45 min at room temperature and then washed. For IFN-γ assays, 4 μg/ml purified anti–IFN-γ capture Ab (clone AN-18; eBioscience) and 1 μg/ml biotinylated anti–IFN-γ detection Ab (clone XMG1.2; BD Biosciences) were used. Supernatants were compared against a standard curve of rIFN-γ standard (PeproTech, Rocky Hill, NJ). All ELISAs were incubated with HRP-conjugated streptavidin (Pierce Endogen; Thermo Scientific) at 0.3 μg/ml for 30 min at room temperature, and then developed using 3,3′,5,5′-tetramethyl-benzidine liquid substrate system (Sigma-Aldrich) and stopped using 0.5 M H_2SO_4. ELISAs were read at 450 nm on a SpectraMax 340PC plate reader and analyzed using Softmax Pro software, both from Molecular Devices (Sunnyvale, CA).

Statistics

The *p* values were obtained using Prism software to calculate unpaired Student *t* tests or, for survival curves, log-rank (Mantel–Cox) tests.

Results

10F.2H11 mAb sterically and functionally blocks only PD-L1: B7-1 interactions, whereas 10F.9G2 blocks both PD-L1:B7-1 and PD-L1:PD-1 interactions

We previously have described a pair of anti–PD-L1 mAbs that have distinct abilities to block the binding of PD-L1 to its two binding partners, PD-1 and B7-1 (16). Based on an in vitro adhesion assay, the 10F.9G2 mAb was found to be a dual blocker, preventing binding of 300.19-PD-L1 transfectants to wells coated with PD-1- or B7-1-Ig fusion proteins. In contrast, the 10F.2H11 mAb blocked adhesion of PD-L1 transfectants to B7-1, but did not impair binding of PD-L1 transfectants to PD-1 fusion protein (16). To further characterize these two anti–PD-L1 mAbs, we first compared their affinities for binding to PD-L1 protein by ELISA, and determined that these two anti–PD-L1 mAbs have comparable affinities for PD-L1 (Fig. 1*A*). When used at the same concentration, 10F.9G2 and 10F.2H11 also similarly stained PD-L1–transfected 300.19 cells (Fig. 1*B*).

We next investigated whether PD-L1 could functionally engage PD-1 when bound by the 10F.2H11 mAb. Despite its inability to block PD-L1:PD-1 binding in adhesion assays, it was possible that 10F.2H11 could bind to PD-L1 in a manner that hindered functional PD-L1:PD-1 interactions. We assessed PD-1 engagement using an in vitro assay with T cells from transgenic mice (PD-1A) that constitutively overexpress PD-1 on T cells (23). In previous studies, we have shown that cocrosslinking of CD3 and PD-1 on PD-1A T cells can inhibit anti-CD3–driven proliferation. We modified this assay and preincubated plate-bound PD-L1 with 10F.9G2 or 10F.2H11 prior to addition of PD-1A T cells. We found that 10F.9G2, but not 10F.2H11, could rescue inhibition of T cell proliferation (Fig. 1*C*). Likewise, 10F.9G2, but not 10F.2H11, rescued the inhibition of IFN-γ production in these assays (Supplemental Fig. 1). Thus, the binding of 10F.2H11 to PD-L1 does not prevent the functional engagement of PD-1 by PD-L1. Therefore, 10F.2H11 can serve as a novel tool to interrogate the function of PD-L1:B7-1 interactions in vivo because it does not disrupt PD-L1:PD-1 interactions and solely affects PD-L1:B7-1 interactions.

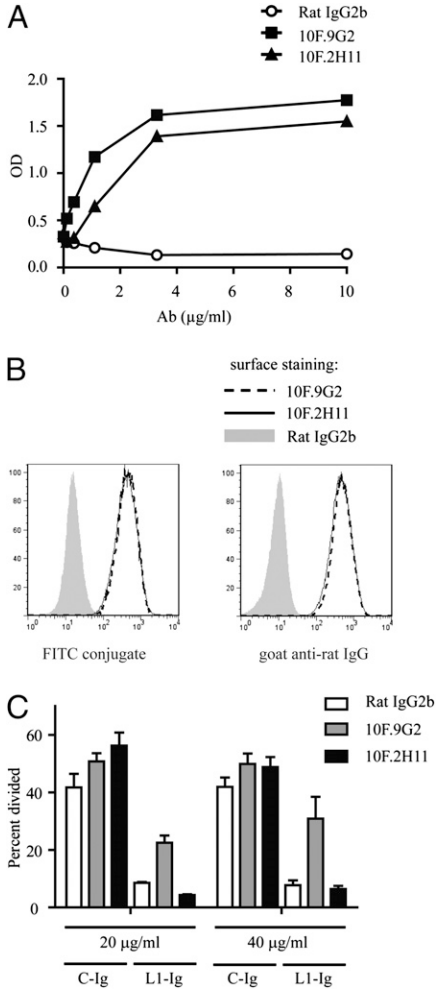

FIGURE 1. Anti–PD-L1 mAb 10F.2H11 does not interfere with functional PD-L1:PD-1 signaling, whereas 10F.9G2 does. *A*, Binding of 10F.9G2, 10F.2H11, and rat IgG2b isotype control mAb to PD-L1-Ig fusion protein was compared by ELISA. *B*, Binding of 10F.9G2 or 10F.2H11 to PD-L1–transfected 300.19 cells assessed by flow cytometry. Directly conjugated mAb (*left panel*) or fluorescently conjugated anti-rat IgG secondary (*right panel*) were used. *C*, Functional engagement of PD-1 is inhibited by 10F.9G2, but not 10F.2H11. PD-1–overexpressing transgenic T cells were cultured on plates coated with anti-CD3 and either PD-L1-Ig fusion protein (L1-Ig) or control protein (C-Ig). After coating, plates were incubated with the indicated concentrations of anti–PD-L1 Abs or control Ab, washed, and then T cells were added. Proliferation was measured by CFSE dilution of 7-AAD–negative T cells by flow cytometry. Data are representative of at least two independent experiments.

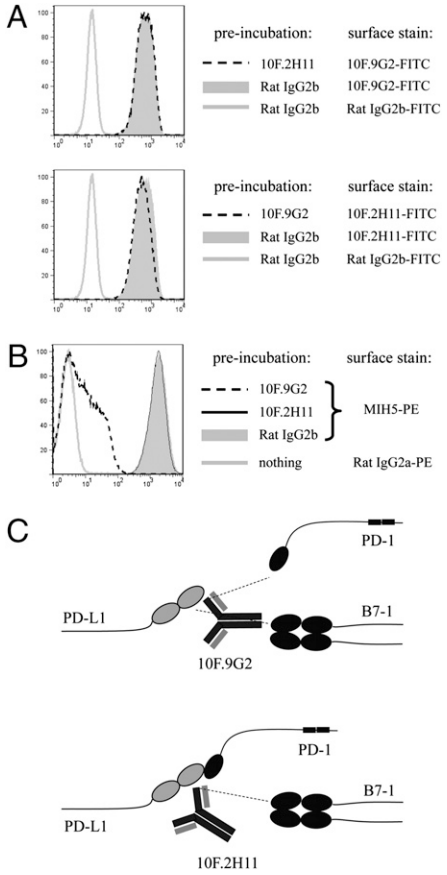

FIGURE 2. The 10F.9G2 and 10F.2H11 mAbs recognize distinct epitopes of PD-L1. *A* and *B*, Analysis of epitopes recognized by 10F.9G2 and 10F.2H11 mAbs. PD-L1–transfected 300.19 cells were preincubated with 20 μg/ml purified Ab and then stained with fluorescently conjugated MIH5, 10F.9G2, 10F.2H11, or isotype control, as indicated. *C*, Schematic depiction of the binding and blocking capabilities of the 10F.9G2 and 10F.2H11 mAbs. Data are representative of at least two independent experiments.

We also assessed whether 10F.9G2 and 10F.2H11 bound to overlapping epitopes on PD-L1. The 300.19-PD-L1 transfectants were preincubated with saturating concentrations of purified 10F.9G2, 10F.2H11, or rat IgG2b isotype control mAb and then stained with fluorescently labeled 10F.9G2 or 10F.2H11 mAb. The 10F.2H11 mAb was not able to block 10F.9G2 binding to PD-L1 and vice versa (Fig. 2*A*), suggesting that 10F.2H11 and 10F.9G2 recognize distinct epitopes on PD-L1. We also compared the abilities of 10F.9G2 and 10F.2H11 mAbs to block the binding of a third anti–PD-L1 mAb, clone MIH5, which, like 9G2 is a dual blocker of PD-L1:PD-1 and PD-L1:B7-1 (A.H. Sharpe and M. Butte, unpublished observations). The 300.19-PD-L1 transfectants were preincubated with saturating concentrations of purified 10F.9G2, 10F.2H11, or rat IgG2b isotype control and then stained with fluorescently conjugated MIH5 Ab. Whereas preincubation with 10F.2H11 mAb had no effect on MIH5 binding, 10F.9G2 preincubation dramatically reduced the level of MIH5 binding (Fig. 2*B*), suggesting that the 10F.9G2 and MIH5 dual blockers bind to overlapping epitopes that are distinct from the epitope recognized by 10F.2H11. We obtained similar data when cells from 10F.9G2- or 10F.2H11-treated mice were stained with MIH5 (data not shown). Our understanding of the binding activities of these two anti–PD-L1 mAbs is depicted in Fig. 2*C*.

10F.2H11 precipitates diabetes in NOD females in an age-dependent manner

We chose to examine the functional significance of PD-L1:B7-1 interactions in the NOD model of autoimmune diabetes because we and others have identified a key role for PD-L1 during the initiation and progression of NOD diabetes (14, 15). In the NOD mouse, disease develops through characteristic stages that begin with peri-insulitis (~3–4 wk of age) and progress to insulitis (~8–10 wk of age). Onset of diabetes occurs in a small percentage of females at ~12–13 wk of age, with incidence approaching 90–100% by 30 wk of age. Because PD-L1 can regulate both the initial activation of potentially pathogenic self-reactive T cells, as well as the responses of pathogenic self-reactive effector T cells in NOD mice, we compared the effect of PD-L1 blockade by administration of 10F.2H11 or 10F.9G2 anti–PD-L1 mAbs to female NOD mice of different ages. We gave the anti–PD-L1 mAbs to nondiabetic 6- to 7- or 13-wk-old NOD mice to compare the effects of these anti–PD-L1 mAbs at early and late phases during the evolution of diabetes. When given to either 6- to 7- or 13-wk-old NOD mice, the 10F.9G2 mAb had profound effects, resulting in diabetes in 90% of the treated mice within 7 d (Fig. 3*A*, 3*B*). In contrast, the 10F.2H11 mAb was significantly less effective than 10F.9G2 ($p = 0.0016$) in precipitating diabetes in 6- to 7-wk-old females, leading to diabetes in 40% of these mice over a 14-d period (Fig. 3*A*). However, 10F.2H11 was almost as effective as 10F.9G2 in precipitating diabetes in 13-wk-old female mice (Fig. 3*B*), resulting in diabetes in 80% of these mice over a 2-wk period. These data demonstrate the PD-L1:B7-1 interaction can inhibit self-reactive T cell responses in vivo. The strong effect of blocking the PD-L1:B7-1 interaction in the older mice suggests that this pathway may be particularly important in restraining effector T cell responses.

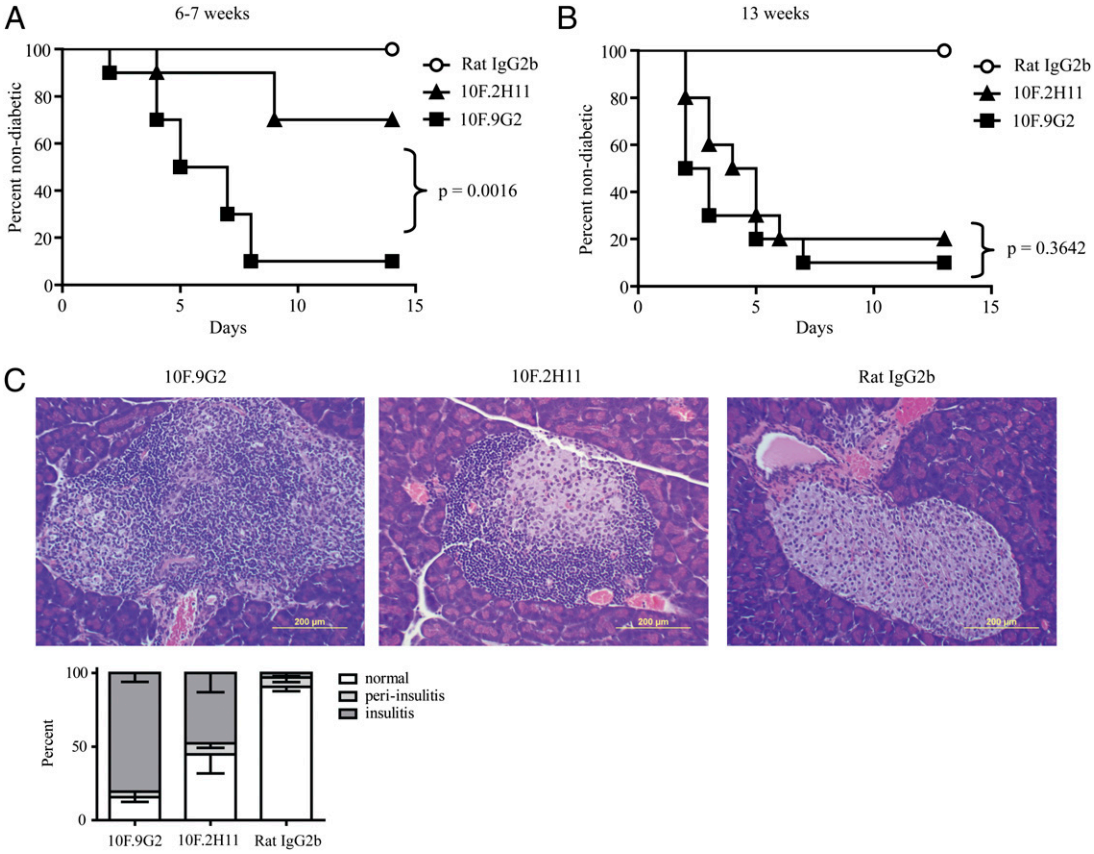

FIGURE 3. The 10F.2H11 mAb precipitates diabetes in NOD females in an age-dependent manner. Six- to 7-wk-old (*A*) or 13-wk-old (*B*) NOD females were treated with 0.5 mg Ab i.p. on day 0, followed by 0.25 mg on days 2, 4, 6, 8, and 10, or until they became diabetic. $n = 10$ for each group; data are representative of three independent experiments. *C*, The 6- to 7-wk-old mice were treated on days 0 and 2, and pancreata were harvested on day 3. H&E stains of representative sections are shown. *Left panel*, 10F.9G2 (insulitis); *middle panel*, 10F.2H11 (peri-insulitis with mild insulitis); *right panel*, rat IgG2b isotype control (no insulitis). Scale bars, 200 μm. Pancreata were scored as either normal (white) or as having peri-insulitis (light gray) or insulitis (dark gray).

We compared the histology of pancreata from 10F.9G2-, 10F.2H11-, or isotype control-treated mice. Pancreata were harvested 2 d after the development of diabetes or, if the mice remained healthy, at 14 d. Pathologic alterations were consistent with clinical manifestations of disease (Supplemental Fig. 2*A*, 2*B*). In the 6- to 7-wk-old mice, insulitis was higher in 10F.9G2-treated as compared with the 10F.2H11-treated mice, but insulitis was comparable in the 10F.9G2- and 10F.2H11-treated 13-wk-old mice. To assess the effects of these two anti–PD-L1 mAbs on T cell infiltration into pancreatic islets at the time when these anti–PD-L1 mAbs have distinct effects, we administered these mAbs to 6-wk-old NOD females twice (days 0 and 2), and then harvested all mice on the following day for histologic evaluation. Pancreata from 10F.9G2-treated mice showed intense insulitis with dense inflammatory infiltrates (Fig. 3*C*). There also were marked infiltrates in pancreata of 10F.2H11-treated mice as compared with isotype control- treated mice, but insulitis was less severe compared with 10F.9G2-treated mice. Insulitis was present in almost 100% of the islets from 10F.9G2-treated mice as compared with 50% from 10F.2H11-treated mice. In isotype control-treated NOD mice, few islets showed peri-insulitis (~6%) or insulitis (~3%). These findings further demonstrate that B7-1:PD-L1 interactions regulate the development of autoimmune diabetes, particularly the progression to insulitis.

T cells from diabetic mice are more susceptible to the effects of 10F.2H11 Ab than T cells from prediabetic mice

To investigate whether 10F.2H11 distinctly affects T cells at different stages of their activation, we used an adoptive transfer approach. We compared the effects of 10F.2H11 or 10F.9G2 mAb administration to NOD SCID recipients of T cells from either prediabetic or diabetic NOD donors. As expected, prediabetic mice had lower proportions of activated T cells than their diabetic counterparts, as defined by CD62L and CD44 surface expression (data not shown). The 10F.9G2, but not the 10F.2H11, mAb accelerated the onset of diabetes such that within 4 wk after transfer, ~50% of recipients of T cells from nondiabetic donors developed diabetes (Fig. 4*A*). However, the 10F.9G2 and 10F.2H11 mAbs similarly accelerated the onset of diabetes in NOD SCID recipients of T cells from diabetic NOD donors (Fig. 4*B*). These findings further support a role for B7-1:PD-L1 interactions in preferentially regulating effector T cell responses. Histological analyses of pancreata from adoptive transfer recipients 10 d after adoptive transfer were consistent with these disease outcomes; insulitis was observed only in 10F.9G2-treated recipients of T cells from prediabetic NOD mice, but in both 10F.9G2- and 10F.2H11-treated recipients of T cells from diabetic mice (Fig. 4*C*, 4*D*). These histologic results suggest that B7-1:PD-L1

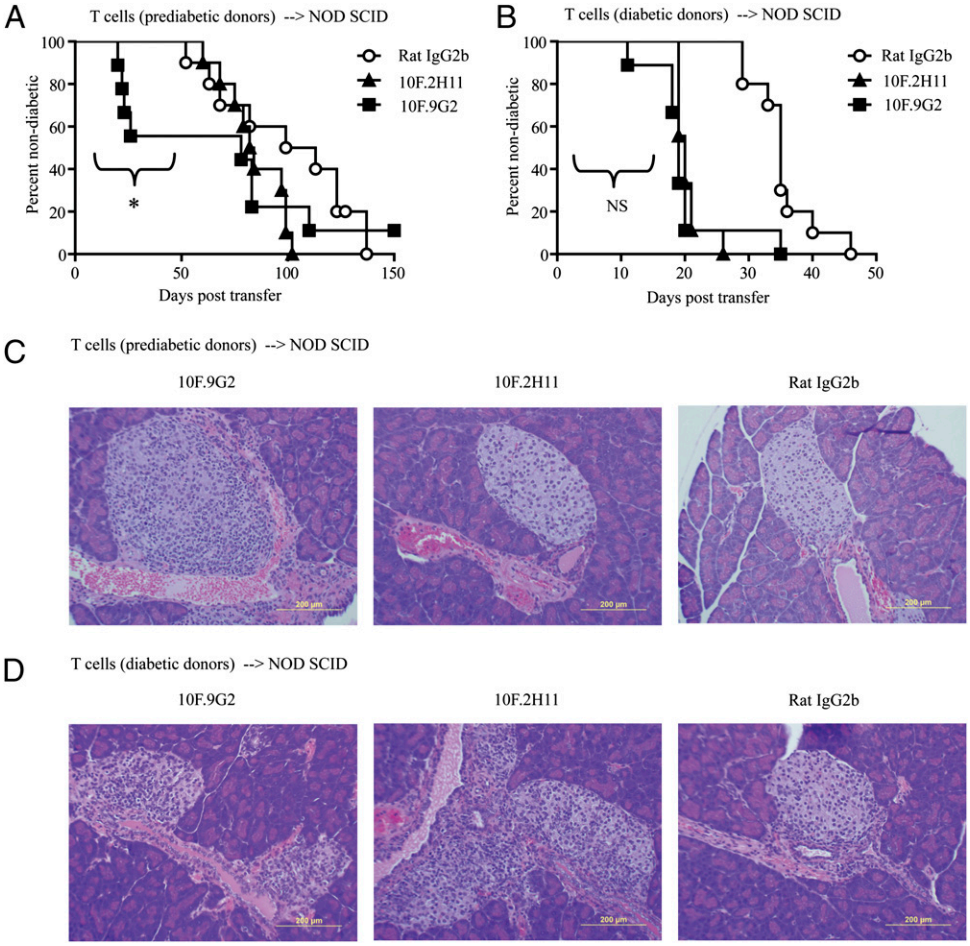

FIGURE 4. T cells from diabetic mice are more susceptible than T cells from prediabetic mice to the effects of 10F.2H11 Ab. $CD4^+$ and $CD8^+$ T cells from prediabetic (*A*) or diabetic (*B*) NOD females were transferred i.v. into NOD SCID recipients that were then treated with 0.5 mg Ab i.p. on day 0, followed by 0.25 mg on days 2, 4, 6, 8, and 10. $*p < 0.05$ over the first 59 d for 10F.9G2 versus 10F.2H11 treatment. For transfers from diabetic donors, the effects of 10F.9G2 versus 10F.2H11 mAb administration were not significantly different over any time frame. Data are pooled from two independent experiments with similar results; n = at least nine per group. Pancreata for histology (H&E) were harvested 10 d after transfer of prediabetic (*C*) or diabetic (*D*) T cells. *Left panels*, 10F.9G2 (insulitis in *C* and *D*); *middle panels*, 10F.2H11 (no insulitis in *C*; insulitis in *D*); *right panels*, rat IgG2b isotype control (no insulitis in *C* or *D*). Scale bars, 200 μm.

interactions influence late diabetes checkpoints. Taken together, these data further demonstrate a functional effect of the PD-L1:B7-1 interaction in vivo, and implicate this pathway in restraining effector T cell function as opposed to priming.

10F.2H11 mAb promotes diabetes following transfer of islet Ag-specific CD4$^+$ and CD8$^+$ effector T cells

We compared the effects of the 10F.9G2 and 10F.2H11 mAbs on diabetogenic CD4$^+$ T cell responses. Diabetes can be transferred to NOD mice by islet Ag-specific effector CD4$^+$ T cells independently from CD8$^+$ T cells. For these studies, we used CD4$^+$ T cells from BDC2.5 NOD mice, which have a TCR from a diabetogenic T cell clone specific for chromogranin A, a pancreatic β cell Ag (25, 26). BDC2.5$^+$ T cells that have been sorted to remove regulatory T cells are able to transfer diabetes to NOD SCID recipients (27). To compare the effects of the 10F.2H11 and 10F.9G2 mAbs on CD4$^+$ T cell-driven diabetes, we transferred BDC2.5$^+$CD4$^+$Foxp3-GFP$^-$ T cells into NOD SCID recipients and gave them either 10F.9G2 or 10F.2H11 mAb. Both anti–PD-L1 mAbs similarly accelerated diabetes onset when compared with isotype control (Fig. 5*A*). These results indicate that B7-1:PD-L1 interactions limit CD4$^+$ T cell–mediated diabetogenesis.

We next examined the effects of 10F.9G2 and 10F.2H11 mAbs in a CD8$^+$ T cell-driven diabetes model. For these studies, we used the 8.3 NOD mouse, which is a TCR transgenic mouse harboring CD8$^+$ T cells specific for a peptide derived from islet-specific glucose-6-phosphatase catalytic subunit-related protein (28). Diabetes in 8.3 NOD mice is partially dependent on the presence of CD4$^+$ T cells, as Rag-2–deficient 8.3 NOD mice develop diabetes later and with lower incidence than Rag-2–sufficient 8.3 NOD mice, and this difference can be reversed by adoptive transfer of nontransgenic NOD CD4$^+$ T cells (28). Consistent with these results, we found that CD8$^+$ T cells from diabetic 8.3 NOD females were only able to transfer disease to NOD SCID recipients with low incidence and late onset (Fig. 5*B*). In marked contrast, administration of either 10F.9G2 or 10F.2H11 mAb to NOD SCID recipients of CD8$^+$ T cells from diabetic 8.3 NOD mice resulted in the rapid induction of diabetes in 100% of the recipient mice (Fig. 5*B*). By day 11 posttransfer, mice were still normoglycemic (data not shown), but CD8$^+$ T cells had infiltrated into islets in 10F.9G2- and 10F.2H11-, but not isotype control-treated mice (Fig. 6). Insulitis was seen in ~25% of islets from 10F.2H11-treated mice and ~40% from 10F.9G2-treated mice, but <4% from isotype control-treated mice.

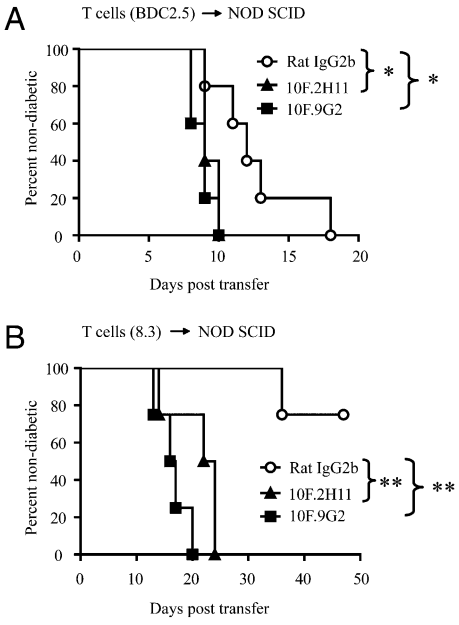

FIGURE 5. Both 10F.2H11 and 10F.9G2 Abs precipitate diabetes transferred by islet Ag-specific transgenic CD4$^+$ or CD8$^+$ effector T cells. A total of 2×10^4 CD4$^+$Foxp3-GFP$^-$ T cells purified from BDC2.5 Foxp3-GFP NOD TCR transgenic mice (*A*) or 4.5×10^6 CD8$^+$ T cells purified from diabetic 8.3$^+$ NOD TCR transgenic mice (*B*) was transferred i.v. to NOD SCID recipients, which were then treated with 0.5 mg Ab i.p. on day 0, followed by 0.25 mg on days 2, 4, 6, 8, and 10. Data are representative of two and four experiments, respectively, each with at least four mice per group. *$p < 0.05$, **$p < 0.005$.

To further assess the effects of the 10F.2H11 mAb on effector T cell responses in NOD SCID recipients of CD8$^+$8.3$^+$ T cells, we treated NOD SCID recipients of CD8$^+$8.3$^+$ T cells with either 10F.2H11 or isotype control mAbs every other day and analyzed them on days 3 and 11 posttransfer. There were no differences in the numbers of cells undergoing cell death, as assessed by 7-AAD staining in splenocytes from isotype control- versus 10F.2H11-treated mice (Supplemental Fig. 3*A*), and the numbers of transferred T cells and recipient dendritic cells were not decreased at any time point analyzed (Supplemental Fig. 3*B*). In fact, in anti–PD-L1–treated mice, CD8$^+$ T cells accumulated in the spleens of anti–PD-L1–treated mice with the absolute number of CD3$^+$CD8$^+$ T cells from 10F.9G2- and 10F.2H11-treated mice being significantly elevated in comparison with isotype control-treated mice by day 11 posttransfer (Fig. 7*A*). Both anti–PD-L1–treated groups displayed increased percentages of activated CD8$^+$ T cells in their spleens compared with isotype control, as defined by low surface expression of CD62L and high surface expression of CD44 (Fig. 7*B*). In addition, CD8$^+$ T cells within both anti–PD-L1–treated groups had higher percentages of IFNγ$^+$TNF-α$^+$ cells (Fig. 7*C*), and the production of these effector cytokines was higher on a per cell basis, as indicated by the mean fluorescence intensity of intracellular stains (Supplemental Fig. 4).

We analyzed the expression of both PD-1 and B7-1 on donor 8.3$^+$ T cells following transfer into NOD SCID mice given isotype control mAb, which were not expected to become diabetic. Expression of PD-1 and B7-1 on donor 8.3$^+$ T cells is low (1–2%) at the time of transfer, and upregulation of these two PD-L1 receptors occurs within days of transfer, with B7-1 being more rapidly expressed. In the spleen, B7-1 is expressed on 22.2% ± 5 of transferred T cells by 3 d posttransfer, whereas only 4.4% ± 0.3 express PD-1 (Fig. 7*D*). The majority of 8.3$^+$ T cells in the spleen that express PD-1 coexpress B7-1. PD-L1 is expressed on ~30% of donor T cells and remains at similar levels over the time frame studied (data not shown). These findings indicate that PD-L1 could engage B7-1 and PD-1 on 8.3$^+$ T cells during the course of anti–PD-L1 mAb administration.

Taken together, our studies indicate that PD-L1:B7-1 interactions can inhibit self-reactive CD8$^+$ effector T cell responses in vivo, and suggest that PD-L1 may restrict "helpless" CD8$^+$ T cell responses (i.e., CD8$^+$ T cell responses generated in the absence of CD4$^+$ T cell help). Thus, using multiple approaches, we find that PD-L1:B7-1 interactions limit potentially pathogenic self-reactive effector T cell responses in vivo.

Discussion

PD-L1 has a key role in controlling the balance between T cell activation and tolerance. We recently identified B7-1 as a second binding partner for PD-L1, and showed that there are bidirectional interactions between B7-1 and PD-L1 that can inhibit T cell responses in vitro (16). In this study, we have demonstrated that the B7-1:PD-L1 pathway plays a role in regulating T cell

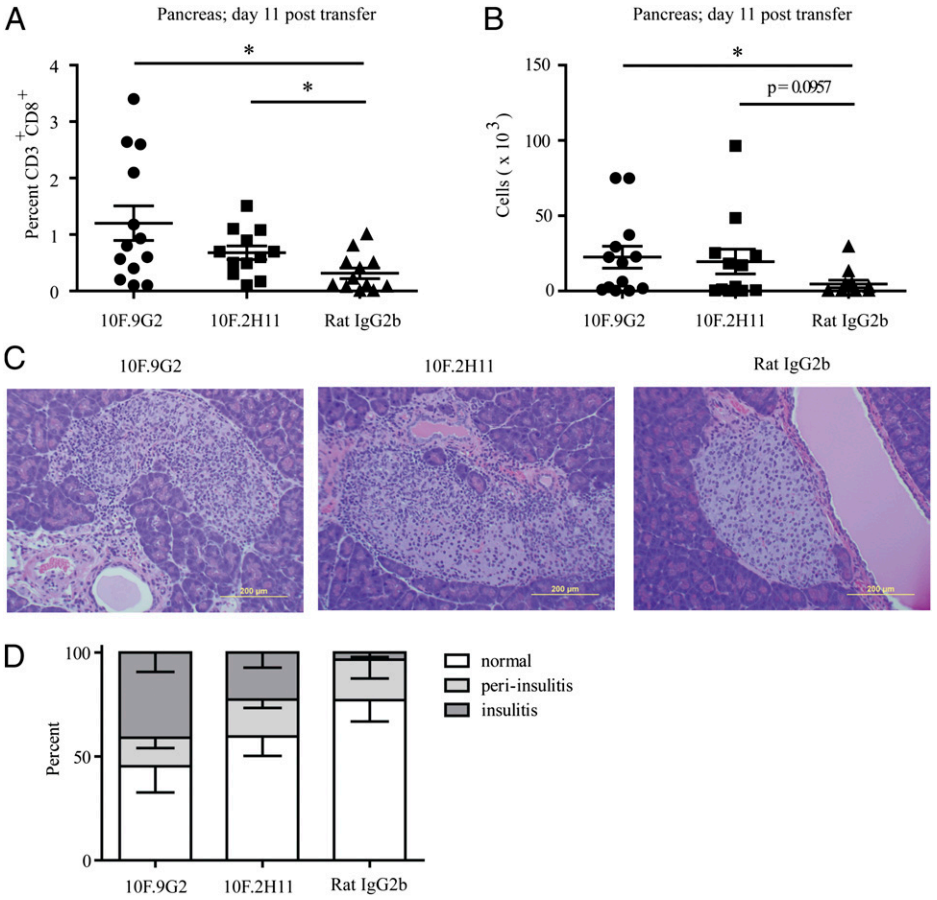

FIGURE 6. Treatment with 10F.2H11 and 10F.9G2 mAb increases islet infiltration by $CD8^+$ effector T cells. NOD SCID recipients of 8.3^+ NOD TCR transgenic T cells were treated with anti–PD-L1 Abs or isotype control and analyzed on day 11 posttransfer. Pancreatic infiltrates were analyzed for the percentage (*A*) and number (*B*) of $CD3^+CD8^+$ T cells. Pooled data from three independent experiments each with at least three mice per group are shown. $*p < 0.05$. Pancreas sections showing islets were stained with H&E (*C*) and scored for insulitis (*D*). *Left panel*, 10F.9G2 (insulitis); *middle panel*, 10F.2H11 (insulitis); *right panel*, rat IgG2b isotype control (no insulitis). Scale bars, 200 μm.

tolerance. We show that this pathway controls the responses of self-reactive T cells in the NOD mouse model of type I diabetes.

The majority of approaches that have been used to analyze PD-L1 function to date cannot discriminate whether PD-L1 is exerting its inhibitory effects by binding to PD-1 or B7-1. We used the novel 10F.2H11 mAb, which we previously identified as a selective blocker of the PD-L1:B7-1 interaction (16), to analyze the function of this interaction in vivo. In this study, we further characterized 10F.2H11 mAb in cross-blocking studies using two anti–PD-L1 mAb, 10F.9G2 and MIH5, both of which can block PD-L1:PD-1 and PD-L1:B7-1 interactions. The 10F.2H11 and 10F.9G2 have similar bivalent affinities for PD-L1, but bind to distinct epitopes on PD-L1, whereas dual-blocker mAbs, MIH5 and 10F.9G2, have overlapping epitopes. We also determined that PD-L1 can functionally engage PD-1 when 10F.2H11 is bound to PD-L1. The cocrystal structure of PD-L1:PD-1 shows that PD-1 binds to the upper part of the GFCC'C" face of the IgV domain of PD-L1 (29). Although the cocrystal structure of PD-L1:B7-1 is not known, the surfaces of PD-L1 that were predicted by chemical cross-linking to bind to PD-1 and B7-1 partially overlapped, with the B7-1–binding surface being somewhat lower on the GFCC'C" face of PD-L1 (16). In PD-L2, the C" and part of C' have been deleted, and if PD-L1 uses this region to bind to B7-1, this may explain why PD-L2 does not bind B7-1 (16, 29–31). Thus, it is plausible that the selective capability of 10F.2H11 to block the B7-1:PD-L1 interaction is due to its binding to PD-L1 in a region, which is necessary for binding to B7-1, but not PD-1.

We compared the consequences of administering the 10F.2H11 and 10F.9G2 anti–PD-L1 mAbs to nondiabetic 6- to 7- or 13-wk-old NOD mice to compare the effects of these anti–PD-L1 mAbs at early and late phases during the progression of diabetes. Although we cannot rule out the possibility that differences in some property of these two rat IgG2b Abs in vivo (such as bioavailability) may lead to quantitative differences in their potencies, we have administered multiple doses at saturating concentrations (data not shown) to attempt to minimize these potential differences. We also evaluated potential effects of 10F.2H11 related to Ab-mediated deletion. Induction of diabetes by 10F.2H11 is unlikely to involve a depleting mechanism such as Ab-dependent cell-mediated cytotoxicity as we did not observe any increase in the numbers of cells undergoing cell death. The numbers of transferred T cells and recipient dendritic cells, both of which might be targets for deletion by virtue of their PD-L1 expression, were not decreased during the course of 8.3^+ T cell adoptive transfer experiments, and, in fact, we observed an increase in the number of transferred T cells in anti–PD-L1–treated mice (Supplemental Fig. 3). In addition, PD-L1–expressing cells were detected ex vivo from 10F.2H11-treated mice at similar levels to isotype control-treated mice using the MIH5 Ab (data not shown).

Although both anti–PD-L1 mAbs could lead to the onset of diabetes in NOD females, the timing of their effects was distinct. When given to either 6- to 7- or 13-wk-old NOD mice, the 10F.9G2 mAb had profound effects, resulting in diabetes in 90% of the treated mice within 7 d. These findings are consistent with a previous study showing that blockade of PD-L1 (using MIH6, which we have found to be a dual blocker; A.H. Sharpe and M.J. Butte, unpublished observations) or PD-1 can accelerate the development of diabetes in NOD female mice (14). Notably, the 10F.2H11 mAb that blocks only the PD-L1:B7-1 interaction led to development of diabetes in 40% of the treated 6- to 7-wk-old NOD mice over a 14-d period, but in 80% of 13-wk-old NOD females within 7 d. The greater effect of 10F.2H11 treatment in

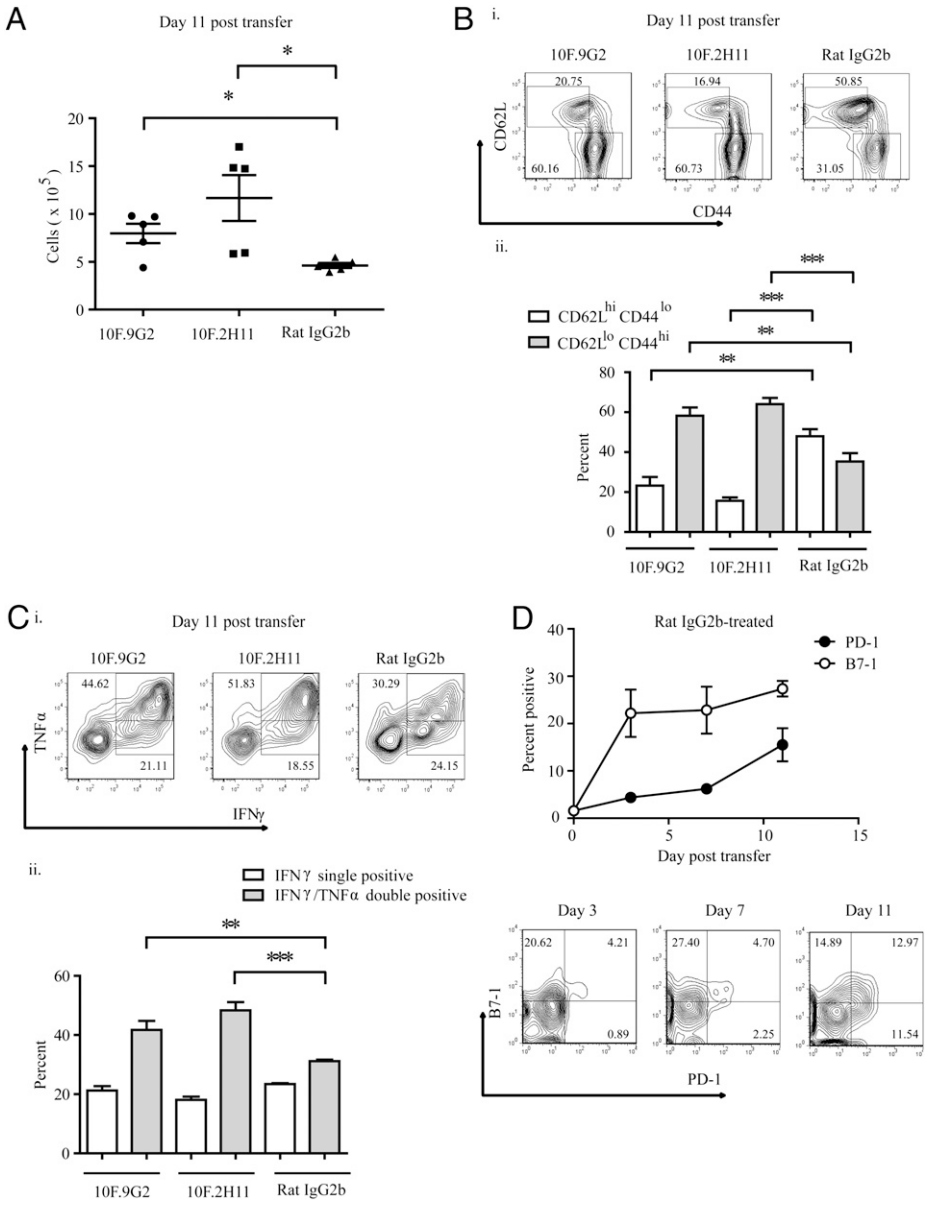

FIGURE 7. The 10F.2H11 and 10F.9G2 mAbs increase $CD8^+$ effector T cell expansion, activation, and cytokine production. NOD SCID recipients were given 8.3^+ NOD TCR transgenic T cells, treated with anti–PD-L1 Abs or isotype control, and analyzed on the indicated day post-transfer. Splenic $CD3^+CD8^+$ T cells were evaluated by flow cytometry for numbers (*A*), activation (*B*), cytokine production (*C*), and B7-1 and PD-1 expression (*D*). *B* and *C*, Representative flow cytometry plots (*i*) and cumulative data (*ii*) are shown. *A–C*, Data representative of three independent experiments, each with five mice per group; *D*, shows representative FACS plots and pooled data from two independent experiments. $*p < 0.05$, $**p < 0.005$, $***p < 0.0005$.

older mice suggests that PD-L1:B7-1 interactions may be particularly important for regulating potentially pathogenic self-reactive effector T cells. To test this hypothesis, we used an adoptive transfer approach to compare the effects of 10F.2H11 or 10F.9G2 mAb administration to NOD SCID recipients of T cells from either prediabetic or diabetic NOD donors. Consistent with our findings in NOD mice, the 10F.2H11 mAb accelerated diabetes in NOD SCID recipients of T cells from diabetic, but not prediabetic, mice. These findings point to a critical role for the PD-L1:B7-1 pathway in inhibiting effector T cell functions in vivo.

In further adoptive transfer studies using BDC2.5 and 8.3 TCR transgenic T cells, we found that 10F.2H11 could accelerate responses of islet Ag-reactive $CD4^+$ and $CD8^+$ effector T cells. The BDC2.5 model is a very rapid and aggressive disease model, in which transferred T cells become rapidly activated in vivo. In the 8.3 model, T cells from diabetic donors, which already have an activated phenotype (data not shown), are transferred. Thus, the equal effect of 10F.2H11 and 10F.9G2 in accelerating or precipitating diabetes in these TCR transgenic models is consistent with a preferential role for PD-L1:B7-1 in controlling the functions of activated effector T cells.

We and others have found that PD-L1 can control peripheral T cell tolerance at multiple checkpoints. PD-L1 can inhibit activation and differentiation of naive self-reactive T cells as well as expansion and functions of effector T cells. Our studies using the 10F.2H11 and 10F.9G2 mAb suggest that the PD-L1:B7-1 interaction primarily restrains self-reactive effector T cells, whereas PD-L1:PD-1 interactions predominate in controlling the initial activation of self-reactive T cells. It may be that the PD-L1:PD-1 pathway is a more potent inhibitory interaction, blockade of which is sufficient to break tolerance at all phases of disease pathogenesis, whereas the PD-L1:B7-1 pathway has a more subtle role. Alternatively, the PD-L1:PD-1 and PD-L1:B7-1 pathways may have overlapping or redundant functions at earlier phases, but unique or nonoverlapping roles after initial T cell activation.

Further studies are needed to understand how the PD-L1:B7-1 pathway exerts its inhibitory functions in vivo. PD-1 and B7-1 are both expressed on activated T cells, and PD-L1 expression is increased on T cells upon their activation. Expression of PD-L1 and B7-1 on activated T cells may explain the predominant function of the PD-L1:B7-1 pathway in controlling effector T cell responses. A recent study using a different single-blocker anti–PD-L1 Ab

showed a role for the PD-L1:B7-1 pathway in a TCR transgenic model of T cell tolerance (32). This study invoked a role for B7-1 on T cells acting as an inhibitory receptor for PD-L1, but was unable to account for the majority of the effects of this Ab, which were independent of the expression of B7-1 on non-T cells and only partially dependent on B7-1 expression on T cells. Using the 8.3^+ T cell adoptive transfer model, we analyzed the expression of both PD-1 and B7-1 on donor 8.3^+ T cells during the course of an adoptive transfer and found that B7-1 is in fact upregulated on donor T cells prior to PD-1. Because the affinity of the PD-L1:B7-1 interaction is lower than that of the PD-L1:PD-1 interaction (16), the existence of a sizeable population of B7-1^+PD-1^- T cells may be an important target of PD-L1–mediated suppression via B7-1 and this population may in turn become the pathogenic population when the PD-L1:B7-1 interaction is blocked. Because both anti–PD-L1 Abs used in our study block the PD-L1:B7-1 interaction, the fact that they have similar effects in this model may be explained by the possibility that the PD-L1:B7-1 interaction predominates in the first days after transfer, prior to upregulation of PD-1.

PD-1 and PD-L1 have become important therapeutic targets because of their key roles in pathogenesis of chronic viral infections, autoimmune diseases, tumor immunity, and transplantation tolerance. Blockade of PD-L1 can enhance T cell responses in the setting of chronic infection or cancer, whereas ligation of PD-L1 has the potential to suppress undesired T cell responses during autoimmunity or transplant rejection. Further work is needed to understand how to effectively manipulate PD-1 and PD-L1 to activate T cells in the setting of chronic infection or tumors, while minimizing the risk of autoimmunity and immunopathology. It may be that single rather than dual blockade will be preferable when modulating PD-L1 under some circumstances. Understanding whether PD-L1:PD-1 and PD-L1:B7-1 interactions have unique or overlapping roles in controlling T cell tolerance and immunopathology may provide insights for effective therapeutic strategies that target PD-L1 and PD-1.

Acknowledgments

We thank Mark Anderson for the gift of 8.3 NOD mice; Rod Bronson and the Dana-Farber Rodent Histopathology Core for assistance with histopathology; Sirisha Tatavarti, Kevin Allan, Flor Gonzalez, and Robert Ortega for technical assistance; and Manish Butte for useful discussions.

Disclosures

A.H.S. and G.J.F. have patents and receive patent royalties related to PD-1. The other authors have no financial conflicts of interest.

References

1. Sheppard, K. A., L. J. Fitz, J. M. Lee, C. Benander, J. A. George, J. Wooters, Y. Qiu, J. M. Jussif, L. L. Carter, C. R. Wood, and D. Chaudhary. 2004. PD-1 inhibits T-cell receptor induced phosphorylation of the ZAP70/CD3zeta signalosome and downstream signaling to PKCtheta. *FEBS Lett.* 574: 37–41.
2. Okazaki, T., A. Maeda, H. Nishimura, T. Kurosaki, and T. Honjo. 2001. PD-1 immunoreceptor inhibits B cell receptor-mediated signaling by recruiting src homology 2-domain-containing tyrosine phosphatase 2 to phosphotyrosine. *Proc. Natl. Acad. Sci. USA* 98: 13866–13871.
3. Keir, M. E., M. J. Butte, G. J. Freeman, and A. H. Sharpe. 2008. PD-1 and its ligands in tolerance and immunity. *Annu. Rev. Immunol.* 26: 677–704.
4. Francisco, L. M., P. T. Sage, and A. H. Sharpe. 2010. The PD-1 pathway in tolerance and autoimmunity. *Immunol. Rev.* 236: 219–242.
5. Dong, H., G. Zhu, K. Tamada, and L. Chen. 1999. B7-H1, a third member of the B7 family, co-stimulates T-cell proliferation and interleukin-10 secretion. *Nat. Med.* 5: 1365–1369.
6. Freeman, G. J., A. J. Long, Y. Iwai, K. Bourque, T. Chernova, H. Nishimura, L. J. Fitz, N. Malenkovich, T. Okazaki, M. C. Byrne, et al. 2000. Engagement of the PD-1 immunoinhibitory receptor by a novel B7 family member leads to negative regulation of lymphocyte activation. *J. Exp. Med.* 192: 1027–1034.
7. Latchman, Y., C. R. Wood, T. Chernova, D. Chaudhary, M. Borde, I. Chernova, Y. Iwai, A. J. Long, J. A. Brown, R. Nunes, et al. 2001. PD-L2 is a second ligand for PD-1 and inhibits T cell activation. *Nat. Immunol.* 2: 261–268.
8. Tseng, S. Y., M. Otsuji, K. Gorski, X. Huang, J. E. Slansky, S. I. Pai, A. Shalabi, T. Shin, D. M. Pardoll, and H. Tsuchiya. 2001. B7-DC, a new dendritic cell molecule with potent costimulatory properties for T cells. *J. Exp. Med.* 193: 839–846.
9. Brown, K. E., G. J. Freeman, E. J. Wherry, and A. H. Sharpe. 2010. Role of PD-1 in regulating acute infections. *Curr. Opin. Immunol.* 22: 397–401.
10. Sharpe, A. H., E. J. Wherry, R. Ahmed, and G. J. Freeman. 2007. The function of programmed cell death 1 and its ligands in regulating autoimmunity and infection. *Nat. Immunol.* 8: 239–245.
11. Zou, W., and L. Chen. 2008. Inhibitory B7-family molecules in the tumour microenvironment. *Nat. Rev. Immunol.* 8: 467–477.
12. Yamazaki, T., H. Akiba, H. Iwai, H. Matsuda, M. Aoki, Y. Tanno, T. Shin, H. Tsuchiya, D. M. Pardoll, K. Okumura, et al. 2002. Expression of programmed death 1 ligands by murine T cells and APC. *J. Immunol.* 169: 5538–5545.
13. Liang, S. C., Y. E. Latchman, J. E. Buhlmann, M. F. Tomczak, B. H. Horwitz, G. J. Freeman, and A. H. Sharpe. 2003. Regulation of PD-1, PD-L1, and PD-L2 expression during normal and autoimmune responses. *Eur. J. Immunol.* 33: 2706–2716.
14. Ansari, M. J., A. D. Salama, T. Chitnis, R. N. Smith, H. Yagita, H. Akiba, T. Yamazaki, M. Azuma, H. Iwai, S. J. Khoury, et al. 2003. The programmed death-1 (PD-1) pathway regulates autoimmune diabetes in nonobese diabetic (NOD) mice. *J. Exp. Med.* 198: 63–69.
15. Keir, M. E., S. C. Liang, I. Guleria, Y. E. Latchman, A. Qipo, L. A. Albacker, M. Koulmanda, G. J. Freeman, M. H. Sayegh, and A. H. Sharpe. 2006. Tissue expression of PD-L1 mediates peripheral T cell tolerance. *J. Exp. Med.* 203: 883–895.
16. Butte, M. J., M. E. Keir, T. B. Phamduy, A. H. Sharpe, and G. J. Freeman. 2007. Programmed death-1 ligand 1 interacts specifically with the B7-1 costimulatory molecule to inhibit T cell responses. *Immunity* 27: 111–122.
17. Butte, M. J., V. Peña-Cruz, M. J. Kim, G. J. Freeman, and A. H. Sharpe. 2008. Interaction of human PD-L1 and B7-1. *Mol. Immunol.* 45: 3567–3572.
18. Ghiotto, M., L. Gauthier, N. Serriari, S. Pastor, A. Truneh, J. A. Nunès, and D. Olive. 2010. PD-L1 and PD-L2 differ in their molecular mechanisms of interaction with PD-1. *Int. Immunol.* 22: 651–660.
19. Latchman, Y. E., S. C. Liang, Y. Wu, T. Chernova, R. A. Sobel, M. Klemm, V. K. Kuchroo, G. J. Freeman, and A. H. Sharpe. 2004. PD-L1-deficient mice show that PD-L1 on T cells, antigen-presenting cells, and host tissues negatively regulates T cells. *Proc. Natl. Acad. Sci. USA* 101: 10691–10696.
20. Keir, M. E., G. J. Freeman, and A. H. Sharpe. 2007. PD-1 regulates self-reactive CD8+ T cell responses to antigen in lymph nodes and tissues. *J. Immunol.* 179: 5064–5070.
21. Wang, J., T. Yoshida, F. Nakaki, H. Hiai, T. Okazaki, and T. Honjo. 2005. Establishment of NOD-Pdcd1$^{-/-}$ mice as an efficient animal model of type I diabetes. *Proc. Natl. Acad. Sci. USA* 102: 11823–11828.
22. Yadav, D., C. Fine, M. Azuma, and N. Sarvetnick. 2007. B7-1 mediated costimulation regulates pancreatic autoimmunity. *Mol. Immunol.* 44: 2616–2624.
23. Keir, M. E., Y. E. Latchman, G. J. Freeman, and A. H. Sharpe. 2005. Programmed death-1 (PD-1):PD-ligand 1 interactions inhibit TCR-mediated positive selection of thymocytes. *J. Immunol.* 175: 7372–7379.
24. Rodig, N., T. Ryan, J. A. Allen, H. Pang, N. Grabie, T. Chernova, E. A. Greenfield, S. C. Liang, A. H. Sharpe, A. H. Lichtman, and G. J. Freeman. 2003. Endothelial expression of PD-L1 and PD-L2 down-regulates CD8+ T cell activation and cytolysis. *Eur. J. Immunol.* 33: 3117–3126.
25. Katz, J. D., B. Wang, K. Haskins, C. Benoist, and D. Mathis. 1993. Following a diabetogenic T cell from genesis through pathogenesis. *Cell* 74: 1089–1100.
26. Stadinski, B. D., T. Delong, N. Reisdorph, R. Reisdorph, R. L. Powell, M. Armstrong, J. D. Piganelli, G. Barbour, B. Bradley, F. Crawford, et al. 2010. Chromogranin A is an autoantigen in type 1 diabetes. *Nat. Immunol.* 11: 225–231.
27. Herman, A. E., G. J. Freeman, D. Mathis, and C. Benoist. 2004. CD4+CD25+ T regulatory cells dependent on ICOS promote regulation of effector cells in the prediabetic lesion. *J. Exp. Med.* 199: 1479–1489.
28. Verdaguer, J., D. Schmidt, A. Amrani, B. Anderson, N. Averill, and P. Santamaria. 1997. Spontaneous autoimmune diabetes in monoclonal T cell nonobese diabetic mice. *J. Exp. Med.* 186: 1663–1676.
29. Lin, D. Y., Y. Tanaka, M. Iwasaki, A. G. Gittis, H. P. Su, B. Mikami, T. Okazaki, T. Honjo, N. Minato, and D. N. Garboczi. 2008. The PD-1/PD-L1 complex resembles the antigen-binding Fv domains of antibodies and T cell receptors. *Proc. Natl. Acad. Sci. USA* 105: 3011–3016.
30. Lázár-Molnár, E., Q. Yan, E. Cao, U. Ramagopal, S. G. Nathenson, and S. C. Almo. 2008. Crystal structure of the complex between programmed death-1 (PD-1) and its ligand PD-L2. *Proc. Natl. Acad. Sci. USA* 105: 10483–10488.
31. Freeman, G. J. 2008. Structures of PD-1 with its ligands: sideways and dancing cheek to cheek. *Proc. Natl. Acad. Sci. USA* 105: 10275–10276.
32. Park, J. J., R. Omiya, Y. Matsumura, Y. Sakoda, A. Kuramasu, M. M. Augustine, S. Yao, F. Tsushima, H. Narazaki, S. Anand, et al. 2010. B7-H1/CD80 interaction is required for the induction and maintenance of peripheral T cell tolerance. *Blood* 116: 1291-1298.